

Comparison of Continuous Performance of a Traction Drive for Different Steel Sheet Measurement Methods

Sven Luthardt¹, Stefan Schmitz¹, Axel Heitmann¹, Dieter Gerling²

¹ *Dr. h.c. F. Porsche AG, Porschestraße 911, 71287 Weissach, sven.luthardt@porsche.de*

² *Lehrstuhl für Elektrische Antriebstechnik und Aktorik, Universität der Bundeswehr München, 85579 Neubiberg*

1 Summary

This paper presents a comparison of continuous performance of a traction motor for a sports car using different electric steel sheet measurement methods. The magnetization curves and the losses are measured with a single sheet tester, an Epstein frame and a ring core. The gathered data is used to fit frequency-based and time-based iron loss model types. With all models the iron losses for the whole operating range of the e-machine are calculated. By using a thermal model of the motor the continuous torque and power are computed. The results show a huge impact on the performance of the electric motor.

Keywords BEV, electric drive, motor design, passenger cars, permanent magnet motor

2 Introduction

The emission laws of vehicle propulsion are going to be more challenging in all important markets in the future [1], so all automobile manufacturers are reacting by launching electric vehicles in the markets. Electrical machines with high speeds, high flux densities and an optimal drivetrain system have to be installed to reach best performance and weight values. Permanent magnet synchronous machines feature certain characteristics such as low rotor losses and high power density, which are important for automobile traction drives. The loss and efficiency maps of the machines are mainly calculated by FEM simulations. Copper losses can be computed easily by the winding resistance, if skin and proximity effects are negligible. Magnet losses and iron losses are calculated after the FEM-simulation in a post processing step. With internal permanent magnet (IPM) machines, especially V-magnet arrangements, rotor iron losses are often higher than magnet losses due to shielding effect in the rotor sheets [2]. Using only a stator cooling jacket, without a rotor cooling, the rotor losses are the dominant loss proportion for the continuous performance of an e-machine [3]. Different iron loss models, as well as the influence of the manufacturing process were often published in the past [4–9]. For example [10] compared different loss models to each other. The investigations are often done for one magnetic curve or different steel grades. In this paper the impact of different steel measurement methods for one steel grade on the continuous performance of a high performance e-machine is shown and compared with a measured curve of a traction drive.

3 Iron sheet measurement methods

There are different possibilities to determine the magnetic curve and the iron losses of an iron sheet used for electric machine design. The magnetic B-H-curve relates directly to the maximum torque of the machine, whereas the loss curves influences the efficiency and the continuous power of the motor. The following sections give a short overview about the most important measurement methods. A detailed description of each method can be found for example in the publication [11].

3.1 Single Sheet Tester (SST)

The first possibility for measuring the magnetic data of an iron sheet is a single sheet tester. The general set-up of a single sheet tester is shown in figure 1.

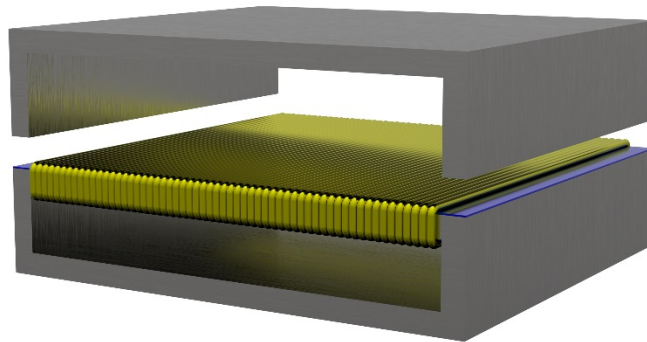


Figure 1: Single sheet tester [11]

The sheet is located in a coil form with a primary and a secondary winding through the two u-form yokes. The sheets should have a minimum length of 500 mm and be almost square. It is easy to measure a sheet in the SST due to the easy exchange of different sheets and the possibility to buy commercial systems. Detailed explanations of the single sheet tester can be found in the DIN IEC 60404-3. The influence of sheet processing on the magnetic properties is very low, because of the huge dimensions of the measured sheet.

3.2 Epstein frame

The second possibility to measure the magnetic data of an iron sheet is to use an Epstein frame. The Epstein frame consists of four square positioned coils with a primary and secondary winding, which are wound around a hollow body. Iron sheets longitudinal and across the rolling direction are stacked together to average the effect of the rolling direction. The width of the sheets should be 30 mm, whereas the length should be between 280-320 mm. The build-up of the Epstein frame is shown in figure 2. The exact specifications can be found in DIN IEC 60404-2. An Epstein measuring system is commercially available and exchanging the samples is very easy. The processing influence is higher than that of the single sheet tester, but not as realistic as in a real machine.

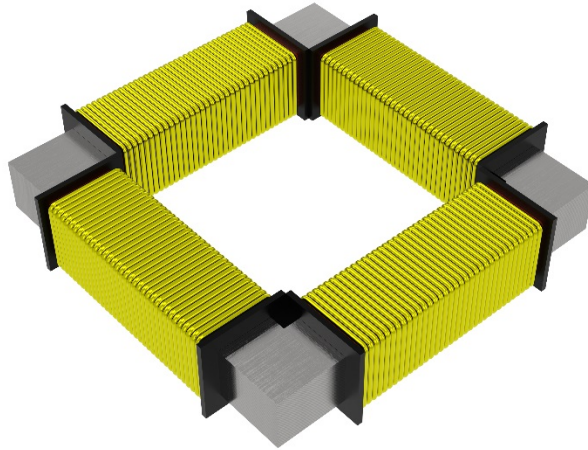


Figure 2: Epstein frame [11]

3.3 Magnetic ring core

The third important possibility to measure the magnetic properties of an iron sheet sample is the magnetic ring core. In contrast to the other two methods, the ring core arrangement offers a closed magnetic circuit. The samples are wound with a primary and a secondary coil. The ratio of outer to inner diameter should be no higher than 1.4, preferably under 1.25. The set-up is shown in figure 3. A detailed explanation of the ring core specification can be found in DIN IEC 60404-6. The preparation of the measurements are labor-intensive compared to the other two possibilities, due to the hand winding of the ring cores. For different frequency ranges several ring cores are necessary. Another problem is the overheating of the samples, caused by the bad thermal connection. Regarding the processing influence, the ring core measurement is the best possibility compared to the machine geometry, especially the yoke and the teeth width of the stator. For a realistic machine design the magnetic data of the ring core measurements should be used.



Figure 3: Ring core [11]

3.4 Magnetic curve and iron losses

For a non-grain oriented 0,2 mm thick steel (NO20) manufactured by ThyssenKrupp the magnetic curve and the iron losses are measured with all three methods. The gathered B-H-curves and the iron losses are shown in figure 4. The magnetic curve of the single sheet tester is better than the results of the Epstein frame and the ring core. This means higher torque in the FEM-calculation, which results from the low processing effect on the material characteristics. The losses of the ring core measurements are much higher than the losses of the Epstein frame and the single sheet tester. It has already been proven that a higher ratio of cut edges to the whole steel area leads to increasing iron losses in the iron sheet material [12]. The consideration of cutting edges by changed material properties of different machine regions in the finite element simulation is published in [13].

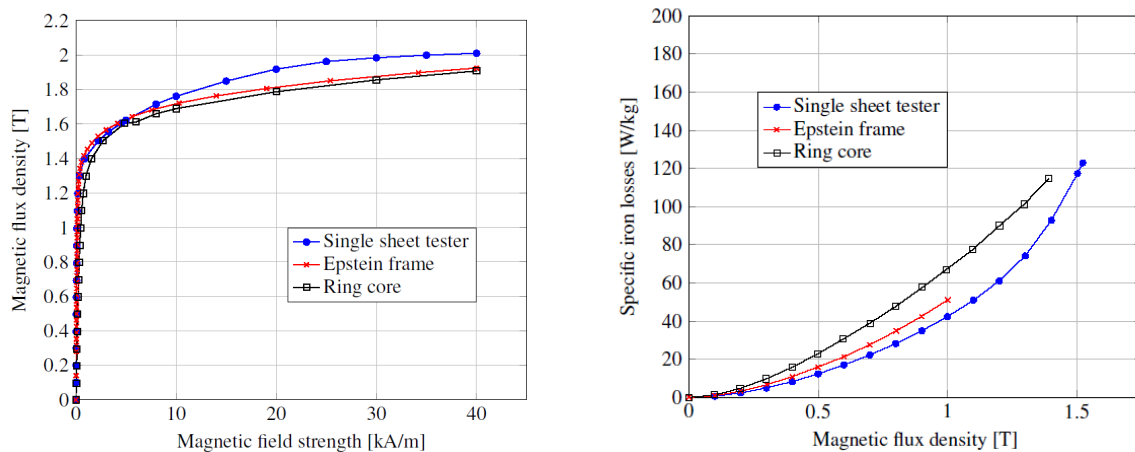


Figure 4: Magnetic properties of NO20 iron sheet for the different measurement methods

On the left the B-H-curve, on the right the iron losses at 1000 Hz supply frequency

4 Iron loss models

With the measured data of the methods described in the last section, the iron loss calculation can be carried out. The calculation of iron losses with a finite element program is done by a post processing step after the computation of the vector potential in each finite element. To use the measured loss curves at frequencies and flux densities, which cannot be directly measured, different iron loss models are known. Several iron loss models are used in the simulation. Generally, these loss models can be divided into frequency-based and time-based models. Frequency based iron loss models are often implemented in simulations with magnetostatic solvers, whereas time based models are more used within transient solvers. In the calculations a 2D-FEM Software using a magnetostatic solver with both iron model types is applied. The following models are implemented:

Frequency based models (FB)

- Steinmetz model
- Jordan model
- Bertotti model (FB)
- IEM-5-parameter model

Time based models (TB)

- Bertotti model (TB1)
- Extended Bertotti model (TB2)

The Bertotti model formulation is used in the frequency and the time domain.

For the Steinmetz model the following equation is used [5]:

$$P_{v,fe} = kf^{\alpha}B^{\beta} \quad (1)$$

The coefficients k , α and β are material dependent and calculated with a mathematical fitting.

The iron losses for the Jordan and the frequency based Bertotti model are calculated with the equations in (2), respectively (3) [14, 15].

$$P_{v,fe} = k_{hyst}fB^2 + k_{eddy}f^2B^2 \quad (2)$$

$$P_{v,fe} = k_{hyst}fB^2 + k_{eddy}f^2B^2 + k_{exc}f^{1.5}B^{1.5} \quad (3)$$

The material parameters k_{hyst} , k_{eddy} , k_{exc} for the hysteresis, eddy and excess losses are determined with a mathematical fitting, for example a Levenberg-Marquardt algorithm.

The IEM model describes the iron losses with the formula in (4) [16], which extent the Bertotti term by a additional saturation-dependent part.

$$P_{v,fe} = a_1B^2f + a_2B^2f^2(1 + a_3B^{a_4}) + a_5f^{1.5}B^{1.5} \quad (4)$$

The parameters a_1 - a_5 could be computed using mathematical, semi-physical or complete physical fitting.

The two time based Bertotti models are implemented with the equation in (5) [17].

$$P_{v,fe} = k_{hyst}fB^2 + \frac{\sigma d^2}{12} \left(\frac{dB}{dt} \right)^2 + \frac{k_{exc}}{8.763} \left(\frac{dB}{dt} \right)^{1.5} \quad (4)$$

Both models have a different complexity regarding the analysis of additional effects such as minor-loops, rotational magnetization or dc-offset in the rotor. The middle term describes the natural eddy current losses, which are dependent on the electric conductivity σ and the thickness d of the iron sheet. The other two parameters are normally calculated by the loss separation principle [18].

5 Thermal network

The thermal model used in the investigation is a 3-dimensional thermal network, modelled in MATLAB [3]. Figure 5 shows the network for the analyzed machine. The machine geometry is discretized in radial and axial direction, to consider different thermal resistances in both axes. This is especially important in the iron sheets and the stator winding. The thermal conductivity in the machine air gap was computed with a CFD-simulation.

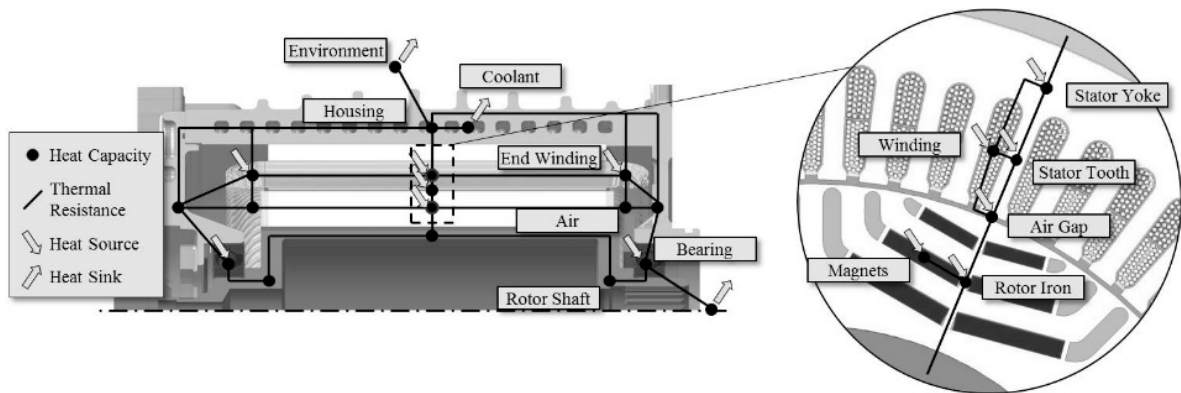


Figure 5: Thermal network of the electric motor [3]

6 Results

With the measured magnetic curves, the losses and the thermal network the loss maps and the continuous performance of a traction motor can be computed as it was done for example in [19]. The main machine data are listed in table 1. The machine is designed for a high power density due to the maximum rotor speed of 15000 rpm. The stator temperature limits are set to 180 °C and the rotor temperatures are limited to 130°C due to demagnetization issues.

Table 1: machine parameters of prototype machine

Dimension	Value
Poles	8
Stator slots	72
Outer diameter	180 mm
Axial length	185 mm
Winding topology	distributed winding
Magnet material	NeFeB
Iron material	ThyssenKrupp NO20
Rotor topology	V-shaped 3 layer
Max. speed	15000 rpm
Nominal DC-voltage	400 V
Cooling	Water-jacket cooled
Stator temperature limit	180 °C
Rotor temperature limit	130 °C

6.1 Comparison of iron loss maps for the measurement methods

For the different measurement methods the iron losses in all machine components are calculated. For a better comparison of the results all losses are calculated with the frequency-based Bertotti model. Figure 6 shows the results for the iron losses in the rotor.

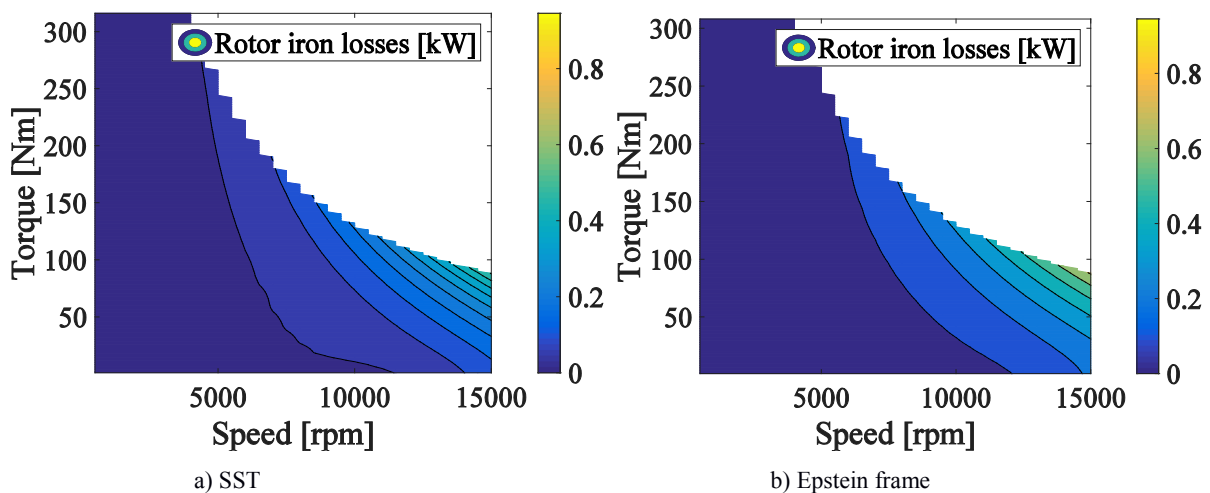


Figure 6: Rotor iron losses for the different measurement methods

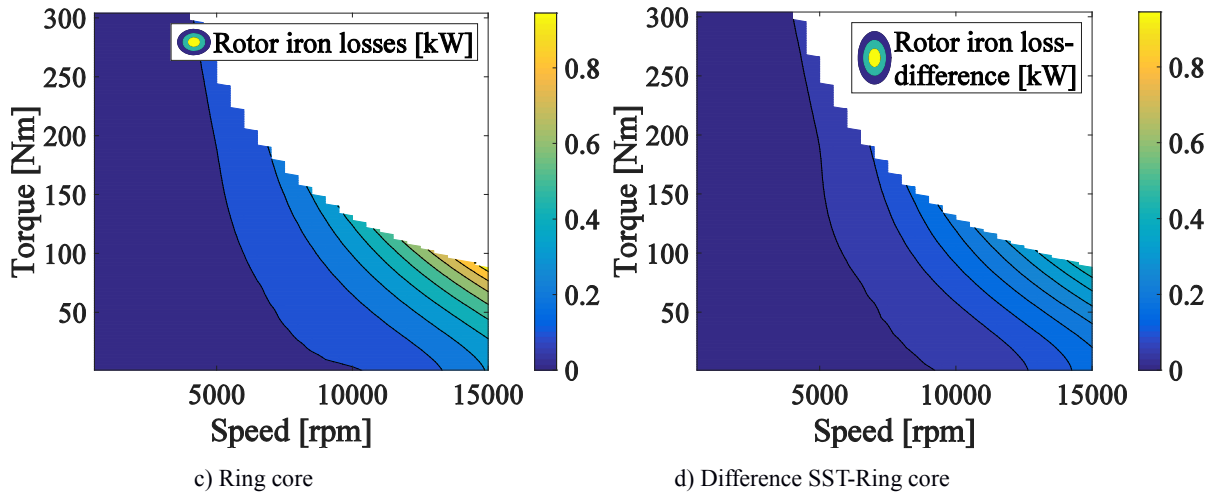


Figure 7: Rotor iron losses for the different measurement methods

It becomes apparent that the iron losses of the single sheet tester are lower than these of the Epstein frame and the ring core. The difference between the ring core and the single sheet tester is approximately 50% of the measured rotor iron losses with the ring core samples. This means a big difference in the calculation of efficiency maps and especially the continuous performance of the electric motor, which is shown in the next section.

6.2 Comparison of loss models

To compare the several iron loss models the continuous performance of the machine is calculated. All results are computed with the data of the ring core measurements. The result is shown in figure 7. The result of the measurement helps to interpret the gathered simulated continuous torque curves. The time based models and the IEM-Model best fits the measured torque, whereas especially the Steinmetz model is not suited for the calculation of this machine. It can be seen that the discrepancy between the measurement and the simulation is at low speed points very high. The explanation is the negligence of the inverter effect in the iron loss and magnet loss calculation, which was investigated in [20, 21]. For highly utilized machine the author of the paper found out that the so called “bathtub” curve in the continuous torque is characteristic. Nevertheless the comparison shows big differences between the various iron loss models.

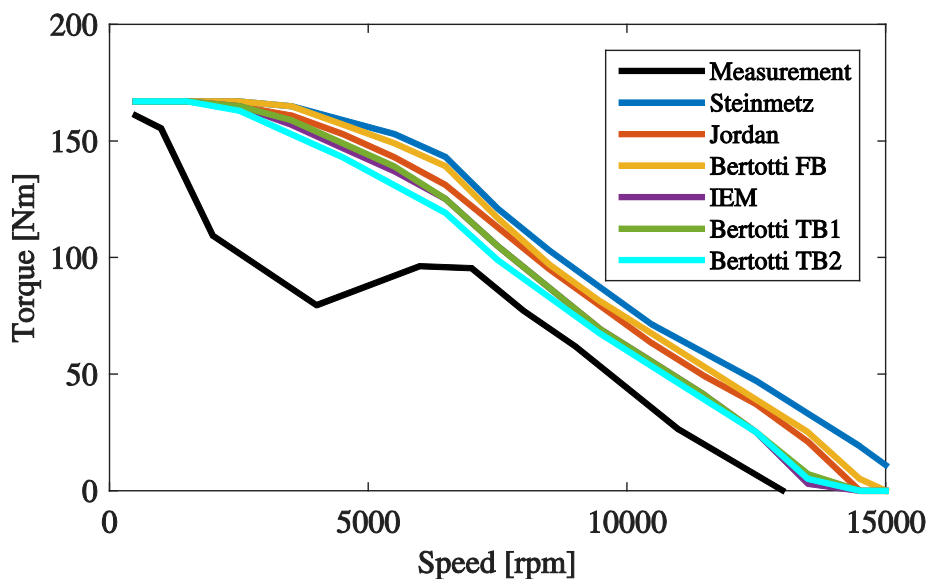


Figure 8: Continuous torque of different iron loss models

7 Test bench setup

To validate the simulation results a prototype machine is built up on a test bench. With the test bench machine from the last section the losses and temperatures for all operating points are measured. The continuous torque and power curves are determined by monitoring all stator and rotor temperatures. Furthermore the maximum torque curve is measured. Figure 9 compares the maximum torque curves of the different methods with the measurement on the test bench. Moreover, the continuous power curve of the measurement is compared to the calculated continuous performance based on the results of the single sheet tester, the Epstein frame and the ring core. The computation with the ring core data shows the best accordance to the maximum torque curve of the measurement on the test bench. After the cutoff rotational speed all datasets have the same development of values. The difference in the rotor iron losses in figure 6 leads to the deviation of the continuous torque curves. The ring core dataset fits best the curve of the test bench, due to the realistic consideration of processing effect in the measurement method.

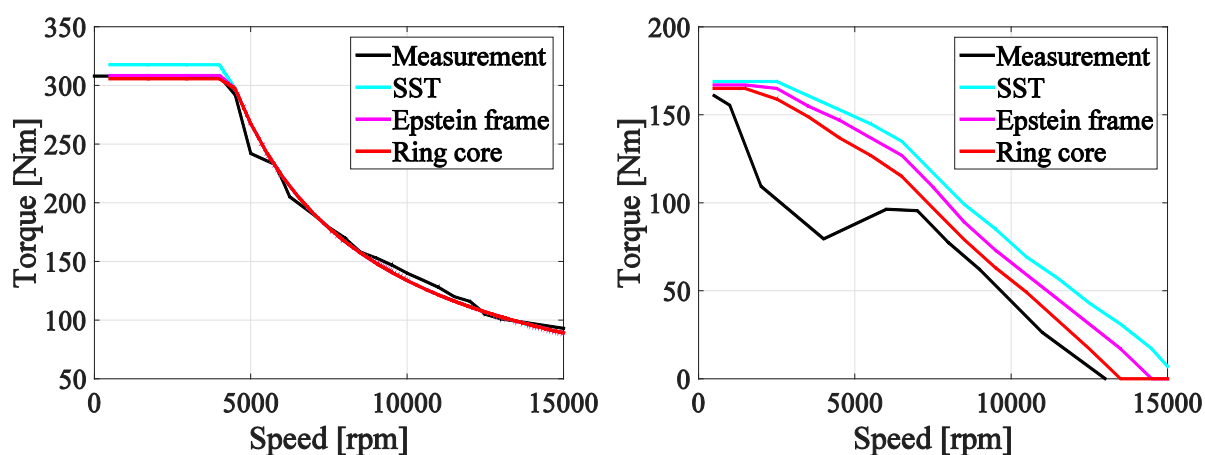


Figure 9: Maximum torque curves and continuous torque of measurement methods

8 Conclusion

Different measurement methods to acquire the magnetic curve and the losses of an arbitrary iron sheet are shown. For the sample iron sheet NO20, the magnetic properties are determined and losses are calculated in the FEM simulation. With the help of a thermal model, which is based on a thermal network, the continuous curves of a traction motor were computed. The iron loss maps and the continuous torque curves show a big influence of measurement methods on the simulation result. To validate the simulation results, a 400 V traction motor was analysed on the test bench. The best fit to the measured data are achieved with the data of the ring core measurement method, due to the realistic shape of iron samples compared to a real machine geometry. It is recommended to use the ring core dataset to consider the processing influence on the magnetic properties of the iron sheet material. Another possibility is using different magnetization and loss curves depending on the distance to the cutting edge, which means a higher measurement and simulation effort [13]. Moreover, the used iron loss model has a big influence on the simulation result. The best curve for the analysed machine in the paper show the time-based models and the IEM-model. The Steinmetz equation is not recommended for highly utilized machines.

References

- [1] T. Puls, "CO₂-Regulierung für Pkw: Fragen und Antworten zu den europäischen Grenzwerten für Fahrzeughersteller," Institut der deutschen Wirtschaft Köln, 2013.
- [2] S. Luthardt, S. Schmitz, A. Heitmann, and D. Gerling, "Improved electric drive analysis methodology for electrical vehicle propulsion," in *European Power Electronics Conference (EPE'16 ECCE Europe)*, 2016.
- [3] S. Oechslen, A. Heitmann, T. Engelhardt, and H.-C. Reuss, "Thermal simulation of an electric motor in continuous and circuit operation," in *16. Internationales Stuttgarter Symposium*, 2016.
- [4] G. Bertotti, *Hysteresis in Magnetism: For Physicists, Materials Scientists, and Engineers*: Academic Press, 1998.
- [5] C. P. Steinmetz, "On the law of hysteresis," *Transactions of the American Institute of Electrical Engineers (AIEE)*, vol. 9, no. 1, pp. 1–64, 1892.
- [6] L. Vandenbossche, S. Jacobs, R. Andreux, N. Labbe, and E. Attrazic, "An innovative approach for the evaluation of iron losses in magnetic laminations, applied to the optimization of highly saturated electric motors," *Inductica Berlin*, 2012.
- [7] S. Steentjes, G. von Pffingsten, M. Hombitzer, and K. Hameyer, "Iron-Loss Model With Consideration of Minor Loops Applied to FE-Simulations of Electrical Machines," *IEEE Transactions on Magnetics*, vol. 49, no. 7, pp. 3945–3948, 2013.
- [8] H. Harstick, "Einfluss des Schneidens auf die magnetischen Eigenschaften von Elektroblech," Dissertation, Technische Universität Clausthal, 2014.
- [9] G. von Pffingsten, S. Steentjes, A. Thul, T. Herold, K. Hameyer, "Soft Magnetic Material Degradation due to Manufacturing Process: A Comparison of Measurements and Numerical Simulations," *17th International Conference on Electrical Machines and Systems (ICEMS)*, pp. 2018–2024, 2014.
- [10] A. Krings and J. Soulard, "Overview and Comparison of Iron Loss Models for Electrical Machines," *Journal of Electrical Engineering*, vol. 10, no. 3, pp. 162–169, 2010.
- [11] A. Böhm, *Messung magnetischer Materialeigenschaften und deren Berücksichtigung bei der Simulation elektrischer Maschinen: zugl. Dissertation an der Universität Erlangen-Nürnberg*. München: Verlag Dr. Hut, 2015.
- [12] L. Vandenbossche, S. Jacobs, F. Henrotte, and K. Hameyer, "Impact of cut edges on magnetization curves and iron losses in e-machines for automotive traction," in *EVS 25 Symposium*, 2010.
- [13] L. Vandenbossche, S. Luthardt, S. Jacobs, S. Schmitz, and E. Attrazic, "Iron Loss modelling of a PMSM Traction Motor, Including the Magnetic Degradation due to Lamination Cutting," in *EVS 30 Symposium 2017*.
- [14] J. Steinbrink, "Analyse von Verlustmodellen und Eigenschaften weichmagnetischer Werkstoffe und deren Einfluss auf die Betriebseigenschaften von PM-Maschinen," *Femag Anwendertreffen*, https://www.profemag.ch/index.php?option=com_phocadownload&view=category&download=354:2011&id=25:2011&Itemid=122, 2011.
- [15] C. Bode, H. May, and W.-R. Candors, "Untersuchung von Wirbelstromverlusten in Permanentmagneten bei hohen Frequenzen: Deutsche Ausarbeitung des Konferenzbeitrags "Optimized reduction of parasitic eddy current losses in high speed permanent magnet motors based 2D and 3D field calculations"," in *XV Int. Symposium on Electromagnetic Fields in Mechatronics, Electrical and Electronic Engineering (ISEF)*, 2011.
- [16] S. Steentjes, D. Eggers, M. Leßmann, and K. Hameyer, "Iron-loss model for the FE-simulation of electrical machines," *Coil Winding, Insulations & Electrical Manufacturing (CWIEME) Berlin*, 2012.
- [17] F. Deng, "An improved iron loss estimation for permanent magnet brushless machines," *IEEE Transactions on Energy Conversion*, vol. 14, no. 4, pp. 1391–1395, 1999.

- [18] E. Barbisio, F. Fiorillo, and C. Ragusa, "Predicting loss in magnetic steels under arbitrary induction waveform and with minor hysteresis loops," *IEEE Transactions on Magnetics*, vol. 40, no. 4, pp. 1810–1819, 2004.
- [19] P. Juris, "Berechnung des Energieverbrauchs und der Temperaturverteilung eines elektrischen Fahrzeugantriebs für charakteristische Fahrzyklen mittels gekoppelter elektromagnetisch thermischer Modelle," *Femag Anwendertreffen*, 2012.
- [20] S. Luthardt, S. Schmitz, A. Heitmann, and D. Gerling, "Analysis of inverter effects on machine iron losses in a traction drive," in *42nd Annual Industrial Electronics Conference (IECON)*, 2016.
- [21] C. Schulte and J. Böcker, "Co-simulation of an electric traction drive," in *IEEE International Electric Machines & Drives Conference (IEMDC)*, 2013.

Authors



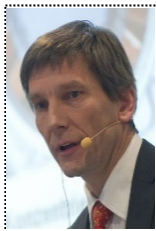
Sven Luthardt was born in 1989 in Sonneberg, Germany. He received the M.S degree in electrical engineering from the University of Erlangen-Nürnberg in 2013. He is currently working towards the Ph.D. degree at Porsche AG, Weissach, Germany in cooperation with the Universität der Bundeswehr München, Neubiberg, Germany. His research interests include the loss analysis of electrical machines for electric vehicle propulsion and the investigation of inverter effects in e-machine simulation process.



Stefan Schmitz was born in 1979 in Waiblingen, Germany. He received the diploma and Ph.D. degrees in electrical engineering from the University of Stuttgart in 2005 and 2010, respectively. In 2010, he joined AMK Arnold Müller GmbH & Co. KG, Kirchheim, Germany as project manager. In 2011, he was with Porsche Engineering Services GmbH, Bietigheim-Bissingen, as development engineer. Since 2012, he has been with Dr. Ing. h.c. F. Porsche AG, Weissach, Germany, as advanced engineering specialist within the advanced engineering drivetrain and electric drives department.



Axel Heitmann was born in 1968 in Erlangen, Germany. He received the diploma and Ph.D. degrees in mechanical engineering from the Technical University of Munich in 1993 and 1998, respectively. In 1999, he joined ZF Friedrichshafen AG, Friedrichshafen, Germany, as advanced engineering specialist. From 2004 to 2012, he was with Audi AG, Ingolstadt, Germany, as advanced engineering specialist and project manager. Since 2013, he has been with Dr. Ing. h.c. F. Porsche AG, Weissach, Germany, as manager advanced engineering drivetrain and electric drives.



Dieter Gerling was born in 1961 in Menden/Sauerland, Germany. He received the diploma and Ph.D. degrees in electrical engineering from the Technical University of Aachen, Aachen, Germany, in 1986 and 1992, respectively. From 1986 to 1999, he was with Philips Research Laboratories, Aachen, as Research Scientist and later as Senior Scientist. In 1999, he joined Robert Bosch GmbH, Bühl, Germany, as Director. Since 2001, he has been a Full Professor at the Universität der Bundeswehr München, Munich, Germany